SCIENTIFIC REPORTS

OPEN

SUBJECT AREAS:
IMMUNITY
PARASITOLOGY
IMAGING
VACCINES

Received
1 April 2011

Accepted
10 June 2011

Published
18 July 2011

Correspondence and requests for materials should be addressed to A.C. (acrs@ic.ac.uk)

Disruption of plasmepsin-4 and merozoites surface protein-7 genes in *Plasmodium berghei* induces combined virulence-attenuated phenotype

Roberta Spaccapelo[1], Elena Aime[1], Sara Caterbi[1], Paola Arcidiacono[1], Barbara Capuccini[1], Manlio Di Cristina[1], Tania Dottorini[1], Mario Rende[1], Francesco Bistoni[1] & Andrea Crisanti[1,2]

[1]Department of Experimental Medicine, University of Perugia, Via Del Giochetto, 06126 Perugia, Italy, [2]Division of Molecular and Cell Biology, Imperial College, Imperial College Road, London SW7 2AZ, United Kingdom.

Blood stage malaria parasites causing a mild and self limited infection in mice have been obtained with either radiation or chemical mutagenesis showing the possibility of developing an attenuated malaria vaccine. Targeted disruption of plasmepsin-4 (*pm4*) or the merozoite surface protein-7 (*msp7*) genes also induces a virulence-attenuated phenotype in terms of absence of experimental cerebral malaria (ECM), delayed increase of parasitemia and reduced mortality rate. The decrease in virulence in parasites lacking either *pm4* or *msp7* is however incomplete and dependent on the parasite and mouse strain combination. The sequential disruption of both genes induced remarkable virulence-attenuated blood-stage parasites characterized by a self-resolving infection with low levels of parasitemia and no ECM. Furthermore, convalescent mice were protected against the challenge with *P. berghei* or *P. yoelii* parasites for several months. These observations provide a proof-of-concept step for the development of human malaria vaccines based on genetically attenuated blood-stage parasites.

Plasmodium falciparum infection causes in non immune individuals a number of life threatening complications including metabolic acidosis, respiratory distress, severe anemia and neurological syndrome known as cerebral malaria that account for the death of about one million children every year in malaria endemic regions. The key pathological features of severe malaria include the obstruction of microvascular districts by parasitized erythrocytes, the rapid expansion of the parasite mass, the destruction of infected erythrocytes and the activation of inflammatory processes[1–3]. The sequestration of parasitized erythrocytes to different vascular districts plays a major role in determining the organs and the tissues affected in some situations such as the brain in cerebral malaria and the placenta in pregnant women[4–8]. Members of the highly polymorphic *P. falciparum* erythrocyte membrane protein 1 family have been shown to play a critical function in this process[9–11]. The role of other factors such as the parasite mass and the growth rate in determining the pathology and the severity of the infection is less clear. Although gene targeting technology has dramatically enhanced our molecular understanding of *P. falciparum* [12–15] blood stage life cycle in terms of its metabolism, growth rate and erythrocyte invasion, the role of individual genes in shaping parasite virulence is much less clear because of the lack of suitable experimental models of human malaria[16–21]. The infection caused by *Plasmodium berghei* in rodents partially mimics human malaria and is regarded as a valuable *in vivo* model to study parasite induced pathology and the development of protective immunity. In *P. berghei*, similarly to what has been observed for *P. falciparum*, disruption of important blood-stage transcribed genes is very difficult to accomplish[22–25]. Only a small number of blood-stage genes, including *msp7* and *pm4*, have been disrupted in both *P. berghei* and *P. falciparum* allowing the analysis of how impairment of *in vitro* growth translates into a virulence change of rodent malaria *in vivo*[23,26–28].

In *P. falciparum* the disruption of the *msp7* gene, a member of a multigene family comprising *msp7* and five *msp7*-related protein (MSRP) genes[29], significantly impairs merozoites invasion of erythrocytes[27]. In the rodent malaria parasites *P. berghei*, that contains a single *msp7* gene and two MSRP genes[23,30], targeting of *msp7* does not induce a dramatic *in vivo* phenotype. These parasites show a more pronounced reticulocyte-tropic cell preference but only a mild growth delay can be observed in infected mice[23]. In *P. falciparum* the disruption of *pm4*, the aspartic protease that functions in the lysosomal compartment and contributes to hemoglobin digestion, causes

only a modest decrease in asexual blood-stage growth rate[26]. Similarly only a modest retardation in the asexual blood-stage growth rate both *in vitro* and *in vivo* is observed in *P. berghei* parasites lacking *pm4*[28]. Surprising this apparently insignificant growth impairment translates into a dramatic decrease in *in vivo* virulence. These parasites failed to induce experimental cerebral malaria (ECM) in ECM-susceptible mice and ECM-resistant mice were able to clear infection. Furthermore, after a single infection all convalescent mice were protected against subsequent challenge with lethal parasites. To further investigate the relationship linking growth rate and virulence we studied the phenotype of Δmsp7 parasites in terms of ability to induce ECM and development of parasitemia in a number of mouse strains with different genetic backgrounds. We have also generated parasites that lack both *msp7* and *pm4* to evaluate if the combined gene disruption had an additive effect on the attenuation of virulence.

Results

Development of MSP7 and PM4/MSP7 knockout *P. berghei* parasites. A parasite strain lacking the *msp7* gene has been already developed few years ago, however because of the need of appropriate controls we generated new parasites clones in which we have disrupted the *msp7* gene in both pbwt (Δmsp7 cl7 and Δmsp7 cl8) and pbwt$^+$ genetic backgrounds[28,31] (Δmsp7$^+$) (Figure 1A). The pbwt$^+$ parasites express a GFP-luciferase fusion protein under the transcriptional control of the *ama-1* promoter that allows the monitoring of parasite load, distribution and patterns of schizont sequestration in live mice by real time *in vivo* imaging. We confirmed the disruption of the *msp7* gene and the correct integration of the replacement construct in all transgenic clones by genomic diagnostic PCR (Figure 1B). Reverse transcription (RT)-PCR (Figure 1C) and immunofluorescence analysis of mixed blood-stage parasites (Figure 1D), from mice with high parasitemia, confirmed the absence of *msp7* transcript and protein in Δmsp7 clones. Double *pm4* and *msp7* knock-out parasite clones (Δpm4/Δmsp7 cl4 and Δpm4/Δmsp7 cl12) were generated from two independent transfection experiments, using a construct designed to target the *msp7* gene in the parasite line Δpm4 cl6 in which the *pm4* gene had been previously deleted[28] (Supplemental Figure 1A). Correct deletion of the *msp7* gene and integration of the replacement construct in the double knock-out parasite was confirmed by genomic diagnostic PCR (Supplemental Figure 1B). The lack of both *msp7* and *pm4* transcripts was showed by RT-PCR analysis from mixed blood-stage parasites (Supplemental Figure 1C).

Virulence phenotype of Δmsp7 and Δpm4/Δmsp7 parasites. We have investigated in different mouse strains the virulence of Δmsp7 parasites in terms of development of peak parasitemia, mortality rate and ability to induce ECM. Mouse strains that are known to be either resistant (BALB/c) or susceptible (C57BL/6 and CD1) to ECM were infected with increasing number of parasites. We observed in Δmsp7 infected BALB/c mice only a mild delay in the parasite growth rate during the initial phase of *in vivo* infection irrespectively of the injection route (intravenous i.v. versus intraperitoneal i.p.) (Figure 2A and 2B). The mice progressively developed a high parasitemia and died during the third week post infection similarly to pbwt-infected mice in agreement with previous reports[23]. The Δmsp7 parasites did not show *in vivo* anomalies in the process of cell maturation and schizont development (not shown). We also extended the characterization of the virulence phenotype of Δmsp7 parasites to ECM susceptible C57BL/6 mice. In this parasite-mouse strain combination, Δmsp7 parasites showed a significant reduction ($p<0.001$) on the growth rate up to day 12 post infection and notably failed to induce signs and symptoms of ECM (Figure 3A, 3C and Supplemental Figure 2A). These mice showed a prolonged course of infection with increasing parasitemia and died during the fourth week post infection with a peak parasitemia reaching 70% (Figure 3A and 3B). On the contrary all pbwt-infected mice died at around day 8 post-infection when the parasitemia was still low (around 20%) developing a typical ECM pathology. Mice inoculated with 10^5 or 10^6 Δmsp7 parasites consistently failed to develop ECM suggesting that the absence of ECM in Δmsp7 infected mice did not depend on the level of parasitemia. The virulence attenuated phenotype Δmsp7 parasites varied with the mouse strain used. A substantial fraction of infected Δmsp7 CD1 mice (about 60%) died within 10 days post-infection with signs and symptoms of ECM and with a parasitemia below 15% while the others mice died later of severe anemia (Figure 3). The parasites in which both *pm4* and *msp7* genes had been disrupted showed irrespective of the mouse strain utilized a remarkable decrease in the virulence that combined the individual phenotypes of the *msp7* and *pm4* knockout parasites. In BALB/c mice the growth rate of Δpm4/Δmsp7 parasites was significantly delayed compared to Δmsp7 parasites up to 12 days post-infection with a peak of parasitemia at around day 21 that was rapidly cleared from the blood resulting in undetectable parasitemia by microscopic analysis by day 30 (Figure 2A and 2B). While C57BL/6 mice infected with single Δpm4 and Δmsp7 parasites did not show any sign of ECM but died later of severe anemia, most of the mice infected with Δpm4/Δmsp7 were able to control and completely clear the parasites from the blood (Figure 3A). Notably Δpm4/Δmsp7 parasites induced in C57BL/6 mice a low peak parasitemia that reached a maximum of 10% at day 12 post-infection and by day 25 the infection became undetectable by microscopic analysis (Figure 3A). On the contrary single *pm4* and *msp7* knock out parasites though failing to cause ECM in C57BL/6 mice consistently induced high levels (up to 70%) of parasitemia. A significant increased on the survival rate was observed in Δpm4/Δmsp7 infected CD1 mice. The majority of the CD1 mice (about 60%) showed a decreased peak of parasitemia, survived the infection and were able to clear the infected red blood cells (iRBCs) by day 30 post-injection (Figure 3). The remaining animals died after day 13 post-infection manly of severe anemia (Figure 3). All these results indicated that virulence phenotype of Δpm4/Δmsp7 parasites was dramatically reduced compared to wild type parasites and combines traits of single *pm4* or *msp7* knock-out parasites.

To further investigate the virulence phenotype of Δpm4/Δmsp7 parasites we infected immunodeficient nude mice that are unable to produce T-cells. Similarly to BALB/c mice all nude animals injected with pbwt infected erythrocytes died within 20 days with high parasitemia (Figure 2C). On the contrary, the mice infected with Δpm4/Δmsp7 survived for more than 50 days and showed low levels of parasitemia in the first four weeks post infection (Figure 2C). Comparable results were also obtained with NOD/SCID mice that carried a combined B- and T-cell immunodeficiency infected with Δpm4/Δmsp7 parasites (data not shown). These findings support previous observation showing that T-cell deficient mice are unable to resolve malaria infections[32]. CD4$^+$ T cells play an important role during the early stages of malarial infection, by amplifying the phagocytic and cell-mediated anti-parasite responses; later in the infection, they help B cells to produce antibodies, and assist in regulating the innate response[33–35].

Analysis of brain pathology in Δmsp7 and Δpm4/Δmsp7 infected mouse strains. The development of cerebral pathology was analyzed in ECM-susceptible C57BL/6 and CD1 mouse strains. In *P. berghei* ECM is a well characterized condition defined as the development of cerebral complications (paralysis, deviation of the head, convulsions, coma) associated with a drop in body temperature to $< 34^{\circ}C$, at day 6–10 after infection[2,36,37]. In this study distinct groups of mice were injected i.p. with 10^5–10^6 pbwt, Δmsp7 and Δpm4/Δmsp7 iRBC. In C57BL/6 mice infected with pbwt we constantly observed clear

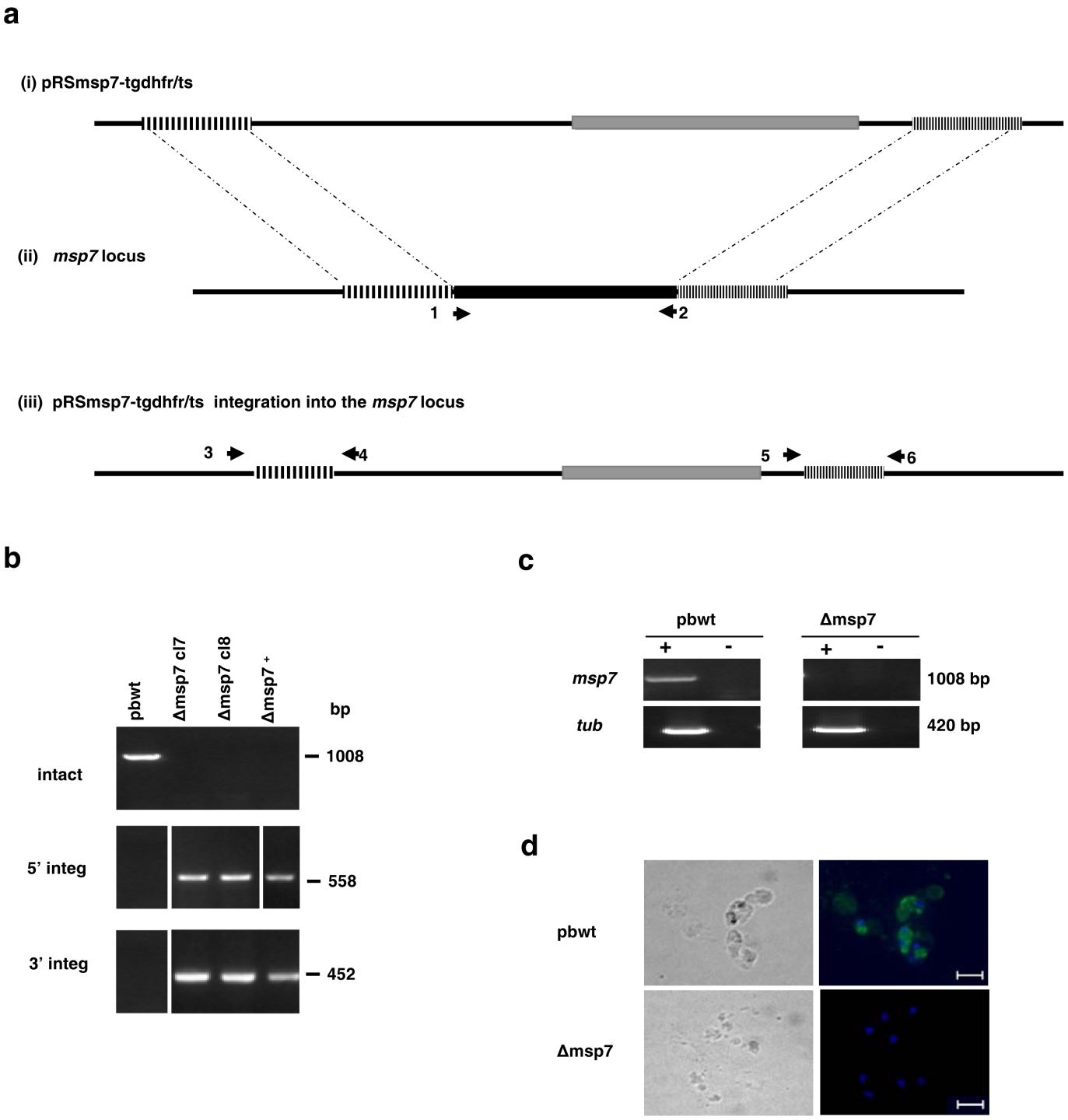

Figure 1 | Targeted gene disruption of the *msp7* locus. (a) Schematic representation of the replacement vector pRSmsp7-tgdhfr/ts (i) and the *msp7* locus (ii). The wild-type *msp7* locus is targeted with a linear fragment containing the 5′ and 3′ UTRs (striped bars) of the *msp7* coding sequence (solid black bars) and the selectable marker *tgdhfr/ts* (gray box). The integration of the construct by double crossover recombination results in the replacement of the *msp7* gene with the *tgdhfr/ts* drug selectable marker (iii). The position and orientation of primers used for diagnostic PCR are indicated with arrow heads. (b) Diagnostic PCR experiments to show the correct integration of the construct. The primer pairs 1+2 amplified a fragment of 1008 bp demonstrating the presence of the intact *msp7* locus in pbwt parasites, whereas no product was obtained with genomic DNA from Δmsp7 parasites clones. The primer pairs 3+4 and 5+6 amplified a product of 558 bp and 452 bp respectively only in the genomic DNA from Δmsp7 parasites demonstrating the correct integration of the construct. (c) In Δmsp7 parasites RT-PCR analysis failed to amplify the *msp7* gene transcript from RNA of blood stage *P. berghei* parasites. As a positive control specific primers were used to amplify the *tub* transcript. (d) Light- and dark- field immunofluorescence microphotographs of pbwt and Δmsp7 parasites analyzed by a polyclonal antibody directed against recombinant MSP7 protein. Bar indicates 50 μm.

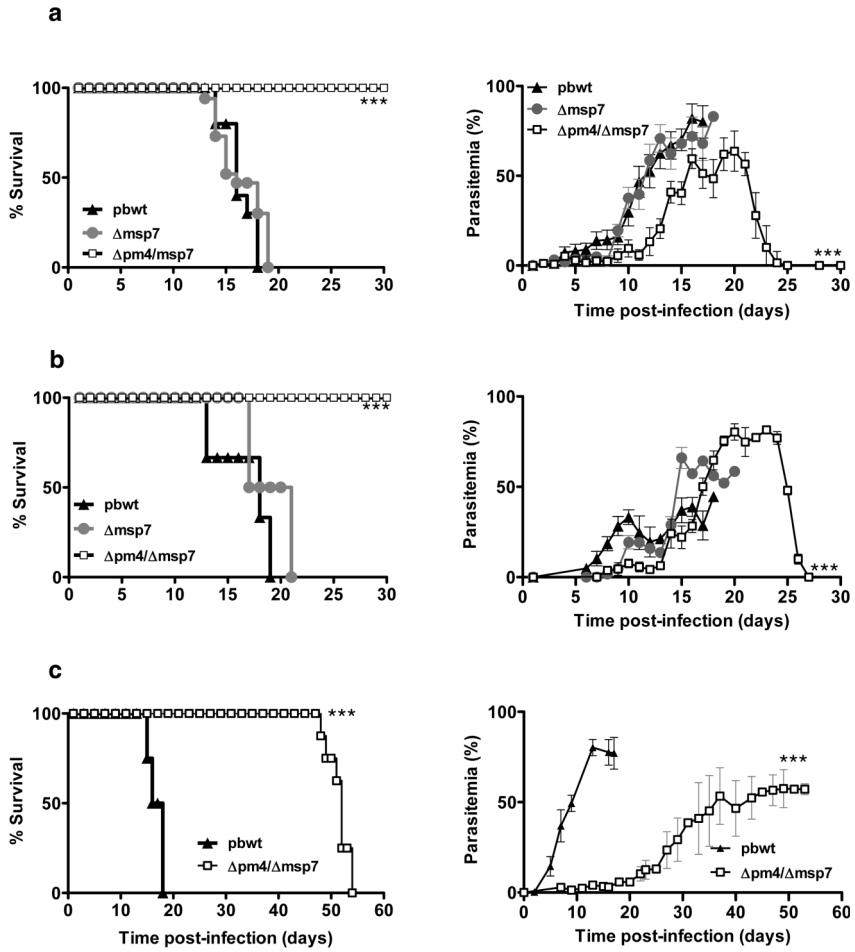

Figure 2 | Time course of Δmsp7 and Δpm4/Δmsp7 infections in BALB/c and nude mice. The percentage of survival (first column) and the time course of parasitemia (second column) are shown. BALB/c mice were inoculated either i.p. (a) (n=10 per group) or i.v. (b) (n=10 per group) with 10^7 and 50 infected erythrocytes respectively using Δmsp7, Δpm4/Δmsp7 and pbwt parasites. Parasitemia was daily evaluated by Giemsa stained thin blood smears. Mice infected with pbwt and Δmsp7 parasites succumbed infection while animals infected with Δpm4/Δmsp7 survived and cleared the infection. (c) Nude mice (n=10 per group) were injected i.p. with 10^7 pbwt or Δpm4/Δmsp7 parasites. In this parasite-mouse strain combination while most of pbwt injected mice died of high parasitemia at around day 20, Δpm4/Δmsp7 injected mice showed very low levels of parasitemia in the first three weeks post-infection and succumbed to the infection only after two months post-injection. These data are representative of 2 two independent experiments. For survival curve log rank test: *** $p<0.001$. For parasitemia Mann-Whitney test between transgenic and wild-type parasites: *** $p<0.001$.

neurological symptoms (such as paralysis, deviation of the head, ataxia, convulsions and coma) associated with a body temperature drop below 34°C suggesting the insurgence of ECM by day seven post infection whereas this outcome was never observed in C57BL/6 mice infected with Δmsp7 or Δpm4/Δmsp7 parasites (Figure 3C). We investigated whether the failure of Δmsp7 parasites to cause ECM was due to a modified sequestration pattern *in vivo*. We analyzed by real time *in vivo* imaging the distribution of schizonts in tissues and organs during infection[28,31,38]. Synchronized $pbwt^+$ (control line) and $\Delta msp7^+$ parasites expressing the luciferase gene under the transcription control of the schizont-specific *ama-1* promoter, injected in CD1 mice showed similar levels of luminescence signal in the lungs, the adipose tissue and the spleen, thus indicating that the disruption of *msp7* did not affect the pattern of schizonts sequestration in these organs and tissues (Supplemental Figure 3). Furthermore $pbwt^+$ and $\Delta msp7^+$ parasites showed a similar timing of peak luciferase activity thus ruling out that the mutant parasite line had a marked impairment of the cell cycle development (Supplemental Figure 3A). For the bioluminescence analysis we infected groups of C57BL/6 mice with increasing numbers of $\Delta msp7^+$ parasites (ranging from 10^5–10^6) and as a control with 10^5 $pbwt^+$ parasites. At 7 days post infection we observed in the brains isolated from $pbwt^+$ infected C57BL/6 mice the presence of a strong bioluminescence signal. In contrast, the brain of $\Delta msp7^+$ infected mice irrespectively of the infection dose and the level of parasitemia showed only a low bioluminescent signal (Figure 4A). Quantitative analysis demonstrated that the observed difference in bioluminescence of $pbwt^+$ or $\Delta msp7^+$ infected brains was significant (Figure 4B). We also investigate the parasites burden during the course of infection in others organs. The results revealed that in CD1 mice $pbwt^+$ parasites are mostly confined in the lungs (50–75%), in the adipose tissues (15–20%) and in the spleen (7–15%) at day 5 post-infection without any relevant variation during the remaining course of infection (Supplemental Figure 2B and 2C). Mice infected with $\Delta msp7^+$ parasites showed the same organ distribution of the bioluminescent signal observed with $pbwt^+$ parasites. An increase of signal in the adipose tissue and in the spleen was observed from day 7 onwards post-infection. We could not carry out a bioluminescence analysis of Δpm4/Δmsp7 parasites because the luciferase reporter is not present in the parasite line. However, we previously reported a significant low bioluminescent signal in the C57BL/6 mice infected with $\Delta pm4^+$ parasites compared to mice infected with $pbwt^+$[28].

To further investigate the development of ECM pathology we examined the integrity of the blood-brain-barrier (BBB) in infected mice using the Evans Blue dye extrusion analysis. Only brains from

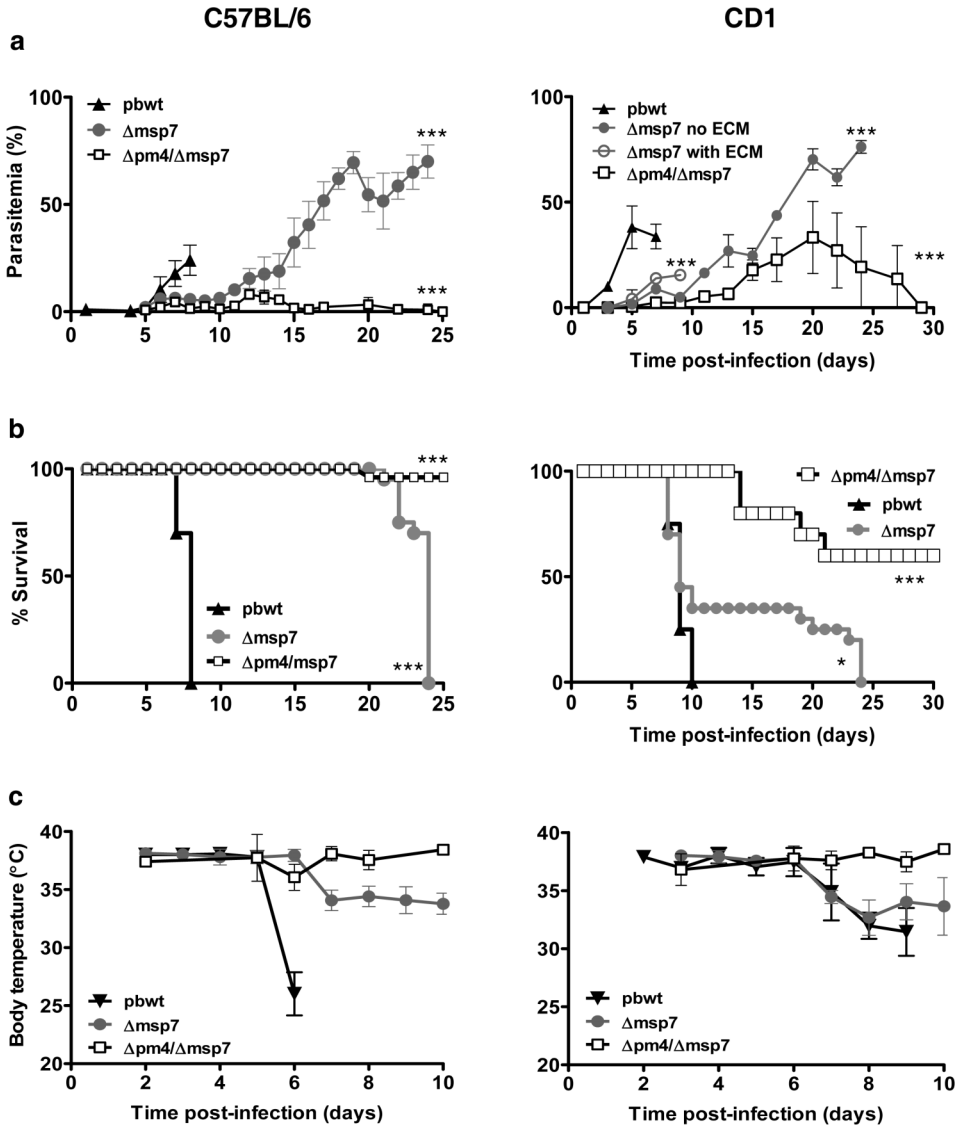

Figure 3 | Time course of Δmsp7 and Δpm4/Δmsp7 infections in C57BL/6 and CD1 mice. The graphs show the level of parasitemia (a), the percentage of survival (b) and the body temperature (c) in C57BL/6 mice (left panel) and CD1 mice (right panel) injected i.p. with 10^5 pbwt, Δmsp7 and Δpm4/Δmsp7 parasites. C57BL/6 mice (n=10 per group) infected with pbwt parasites died approximately 6–8 days post infection showing low level of parasitemia (below 20%) and signs of ECM accompanied with hypothermia. On the contrary mice infected with Δmsp7 parasites did not show signs of ECM, survived up to the forth week post infection and died shortly afterwards with very high parasitemia. Mice infected with Δpm4/Δmsp7 did not show signs of ECM, develop lower levels of parasitemia compared to pbwt and Δmsp7 parasites and cleared the infection by day 25. CD1 mice infected with pbwt parasites died between day 8 to 12 post infection with a parasitemia of about 40% showing sign and symptoms of ECM. Some mice (around 40%) infected with Δmsp7 parasites did not developed ECM and died within the third week post infection with high parasitemia. Most of the mice (60%) infected with Δpm4/Δmsp7 parasites neither did developed neurological signs nor showed any drop in the body temperature. The animals that survived infection showed lower levels of parasitemia compared to single Δmsp7 parasites and cleared the infection by day 30 post infection. The levels of parasitemia of CD1 mice infected with Δpm4/Δmsp7 represent the mean ± SD from only the mice that survived infection. These data are representative of 2 two independent experiments. For survival curve log rank test: * $p<0.05$, *** $p<0.001$. For parasitemia Mann-Whitney test between transgenic and wild-type parasites: *** $p<0.001$.

pbwt$^+$ infected animals showed a clear blue color after perfusion that was almost absent in the brains of mice infected with Δmsp7 and Δpm4/Δmsp7 (Figure 4C). The quantification of Evans Blue in the brains extract demonstrated that the infection with Δmsp7 and Δpm4/Δmsp7 contrary to pbwt caused little damage to the BBB (Figure 4D).

Δpm4/Δmsp7 infection induces a long lasting protective immunity in convalescent mice. BALB/c, C57BL/6 and CD1 mice that had recovered from infection after a single injection of Δpm4/Δmsp7 parasites were challenged with pbwt iRBCs. All mice strains tested were protected against lethal parasite challenge given at high doses of 10^7 (Table 1). Challenged mice showed a short-lasting and low level parasitemia of <0.01% that was usually cleared within 10 days. The protection elicited by double knockout parasites was monitored for up to six months after recovery from the initial infection. We also performed sub-inoculation of blood from challenged animals into naïve mice (n=10) and none of them developed a detectable parasitemia by microscopic analysis. Immunized mice were also challenged with a different rodent malaria parasite species *P. yoelii*. The immune response induced by Δpm4/Δmsp7 parasites protected the mice also against the heterologous challenge with 10^4 *P. yoelii*

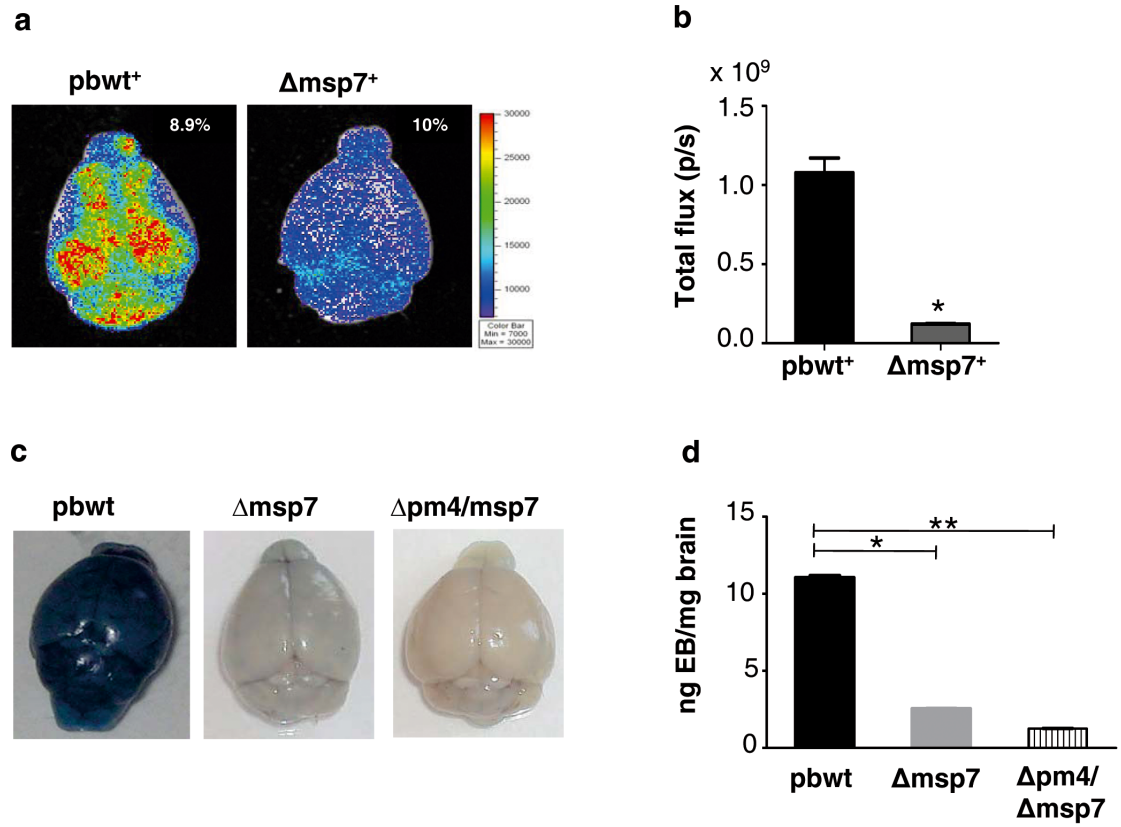

Figure 4 | Parasite distribution and blood vessel permeability in C57BL/6 infected mice. (a) Representative bioluminescent images of 7 days post infection brains isolated from C57BL/6 mice infected with either pbwt$^+$ or Δmsp7$^+$ parasites. The level of parasitemia at the time the brains were collected is shown as percentage in the photograph panels. (b) Quantitative analysis of the luminescence signal collected from the brains of mice infected with either pbwt$^+$ or Δmsp7$^+$ parasites. Mann-Whitney test: * $p<0.05$. (c) Representative digital images of Evans Blue dye extrusion analysis of brains from pbwt, Δmsp7 and Δmsp7/Δmsp7 infected C57BL/6 mice collected at day 7 post-infection. Only pbwt infected animals showed a blue staining post infusion with Evans Blue dye that was nearly absent in the brains of Δmsp7 or Δmsp7/Δmsp7 infected mice. (d) Quantitative analysis of Evans Blue staining of brains from infected mice (n=6). Bars represent the mean ± SD from 6 mice. Mann-Whitney test: * $p<0.05$, ** $p<0.01$.

iRBCs (Table 1). Challenged mice failed to develop a detectable infection by microscopic analysis.

Discussion

We show here that Δmsp7 parasites carrying a disrupted *msp7* gene, a mutation previously reported to cause a modest growth delay, have a virulence attenuated phenotype. When injected to ECM susceptible C57BL/6 mice Δmsp7 parasites did not induce signs or symptoms of cerebral malaria. At 7 days post-infection the brains of C57BL/6 mice infected with Δmsp7$^+$, a parasite line that carries a disrupted *msp7* and expresses the luciferase gene under the transcription control of the blood stage promoter *ama-1*, showed a much lower bioluminescent signal than the brains of pbwt$^+$ infected mice. Furthermore unlike pbwt, the infection caused by Δmsp7 parasites did not damage the blood brain barrier (BBB) as demonstrated by the distribution of Evans Blue dye in isolated perfused brains. The ECM virulence phenotype of Δmsp7 parasites is very similar to that observed in *P. berghei* after disrupting the aspartic protease plasmepsin 4 gene[28] thought *msp7* and *pm4* are functionally unrelated. Parasites lacking either *pm4* or *msp7* have in common a mild impairment of the *in vivo* growth. Possibly a reduction in the parasite growth rate and hence in the parasite mass as well as in the products of parasite metabolism may affect both the magnitude and the cytokine profile of the immune response that in turn determine the occurrence of ECM in susceptible animals. The recent observation that an imbalance of the anti-inflammatory molecule heme oxygenase (HO)-1 and its substrate heme (a product of hemoglobin degradation) has a role in triggering ECM would support this notion[39]. Indeed evidence originated from other rodent malaria parasites suggests that growth delay or drug mediated arrest in the erythrocytic cycle could translate into a significant reduction of virulence and in the induction of protective immunity. As an example in *P. yoelii* the disruption of the gene encoding the purine nucleoside phosphorylase (PNP) caused a significant reduction of parasite growth and caused a self limiting infection *in vivo*[40]. Similarly, in this parasite species the disruption of the nucleoside transporter 1 (NT1) generated severely attenuated blood-stage parasites that conferred complete sterile protection against

Table 1 | Protection of Δpm4/Δmsp7 immunized mice against challenged with *P. berghei* or *P. yoelii*.

Mouse strain	Challenge	Time of challenge (days)*	Challenge dose (no. of parasites)†	No. protected/ challenged
BALB/c	*P. berghei* (ANKA)	0	10^7	0/10
BALB/c	''	140	10^7	14/14
C57BL/6	''	0	10^7	0/10
C57BL/6	''	190	10^7	10/10
CD1	''	0	10^7	0/10
CD1	''	150	10^7	10/10
BALB/c	*P. yoelii* (17X)	0	10^4	0/10
BALB/c	''	30	10^4	10/10

*Number of days after recovery from first infection with Δpm4/Δmsp7 parasites.
†Mice were challenged by i.v. injection of iRBCs

subsequent challenges with lethal parasites[41]. Furthermore, experiments conducted on drug treated infected mice have shown that timing and antigen dose play a critical role on the development of an immune response[42–44]. These studies have highlighted the potential importance of the early events in priming an immune response and also the possible immunosuppressive effect of high levels of parasitemia. Recent clinical studies indicate that a strong immune protective response could be elicited by drug cure low dose of both *P. falciparum* iRBCs or sporozoites[45,46]. However a reduced parasite growth rate is not invariably associated with an attenuated ECM virulence phenotype. *P. berghei* parasites lacking the elongation factor 1a (eef1a) have a slow growth rate due to a prolonged G1 phase[22], but induce ECM in susceptible mice. Similarly cathepsin C knockout parasites grow slower *in vivo* than the pbwt parental strain but are able to induce ECM (unpublished observations RS).

With respect to the ability to reach sustained levels of parasitemia Δmsp7 and Δpm4 parasites showed distinct phenotypes that varied with the mouse strain utilized. In BALB/c mice, Δpm4 parasites caused a self-resolving infection while in ECM susceptible C57BL/6 and CD1 mice these parasites though failing to induce ECM progressively reached a high parasitemia and caused the death of the animals[28]. Irrespectively of the mouse strain utilized Δmsp7 parasites did not cause a self-resolving infection. The number of parasites in the blood increased progressively until the death of the animals. Notably the disruption of both *pm4* and *msp7* genes generated parasites that compared to the individual knockout strains showed a more dramatic virulence attenuated phenotype that this time did not vary with the genetic background of the mice. Irrespective of the mouse strains utilized Δpm4/Δmsp7 parasites generally caused a self-resolving infection that in a substantial fraction of the infected mice was also characterized by a drastic reduction of the parasitemia. Furthermore Δpm4/Δmsp7 parasites failed to induce ECM in susceptible mouse strains similar to what we observed in individual knockout parasites. The self-resolving infection caused by double knockout parasites was accompanied with a strong and long lasting protective immune response against subsequent challenge with homologous and heterologous parasites. Previous experiments conducted with Δpm4 parasites have indicated that antibodies play a crucial role in the protection elicited in these experimental models[28].

In this paper, we utilized the available knowledge and properties of *P. berghei* iRBCs sequestration and used the recent advances in *in vivo* imaging technologies to visualize parasite distribution and load in different organs of live mice infected with pbwt$^+$ and Δmsp7$^+$ parasites that express luciferase gene under the control of a schizont-specific promoter (i.e., the *ama*-1). Imagings performed in experimentally induced synchronous infections in mice were established by injection of 0.5 to 1×10^8 purified mature schizonts in four mice[31]. Collection of data at 21–23h after injection allowed the visualization of sequesters parasites only in the lungs, adipose tissue and the spleen[28,38]. The luck of bioluminescence signal in the brain could be due to several factors ranging from low level of parasites, below the detection limit of the instruments, or to others factors such as putative endothelial receptors expression, inflammatory markers and adhesins that became up-regulated during infection. While blood parasitemia has been routinely used to monitor disease progression, it is now recognized that measurements of total parasite biomass in the whole body offer a better correlate of the disease status of malaria patients. Bioluminescence analysis of complete mice or organs from different animals during ongoing infections can be compared quantitatively and use to evaluate parasites burden. Several recent studies have shown by in vivo imaging that the timing of this iRBCs accumulation in the brain coincides with the development of ECM and mice protected from cerebral complications do not show a similar increase of iRBCs sequestration in the brain[28,38,47,48]. Anyway, bioluminescence alone could not be use to define precisely the parasites burden in some organs (i.e., brain) and further analysis are required. Parasites expressing different fluorescent reporter proteins (e.g., GFP and mCherry) now offer the possibility to provide an insight into the amounts of parasites (i.e., load) that accumulate into the organs to understand malaria pathology by, for example, using multiphoton microscopy.

The enhanced virulence attenuation phenotype observed of Δpm4/Δmsp7 parasites bears crucial implications for the development of a malaria vaccine. The lack of significant progress with subunit vaccines that contain only (parts of) single proteins, together with an enhanced understanding of the protective immunity to malaria has generated new interest in vaccines based on whole blood stage parasite[49]. Sporozoites that have been attenuated either by radiation or by genetic modification have shown promise as a whole parasite approach to pre-erythrocytic vaccination[50–55]. Recent studies have demonstrated that the disruption of individual genes was not sufficient to completely attenuate parasite virulence. Infection with p52-deficient sporozoites protected mice against subsequent infectious sporozoite challenge, but the immunizations led to sporozoite dose-dependent breakthrough infections[56,57]. On the contrary sporozoites lacking both p52 and p36 exhibited a complete growth arrest in the liver *in vitro*[58]. This study now demonstrates that sequential disruption of specific blood-stage genes generates blood-stage parasites with a progressively virulence-attenuated phenotype that are capable of inducing protective immunity in the *P. berghei* model of malaria. These observations provide a compelling case for generating additional genetically attenuated blood stage (GABS) mutants for assessing their potential usefulness in the development of GABS based human malaria vaccines.

Methods

Mice and parasites. Six- to eight-week-old female C57BL/6 were purchased from Charles River while CD1, BALB/c and nude mice were purchased from Harlan Sprague. NOD/SCID (age 10–16 weeks) were kindly provided by Prof. Velardi and Prof. Falini. All studies involving animals have been performed according to the D.L 27 January 1992, n. 116, Italian legislation. The parasite strain *P. berghei* ANKA was used as a control for wild type parasite (pbwt) and for the generation of the mutant lines Δmsp7 cl7 and Δmsp7 cl8. The *msp7* gene (PBANKA_134910) has been disrupted by introducing the construct pRSmsp7-tgdhfr/ts into the genome of pbwt parasites by double cross-over recombination as described below. Clones Δmsp7 cl7 and Δmsp7 cl8 were obtained from two transfection experiments. Δmsp7$^+$ is a mutant parasite line (Δmsp7 cl9) generated introducing construct pRSmsp7-tgdhfr/ts into the genome of pbwt$^+$ parasites by double cross-over recombination. The parasite strain pbwt$^+$ (1037cl1) is a reference transgenic parasite line that expresses a fusion protein (GFP-Luc) encompassing the GFP (mutant3) and the luciferase (LUC-IAV) coding sequence under the control of the schizont-specific *ama-1* promoter[28]. Δpm4/Δmsp7 cl4 and Δpm4/Δmsp7 cl12 are two mutant parasite clones that are deficient in both *pm4* and *msp7* genes obtained by introducing pRSmsp7-hdhfr construct into the genome of Δpm4 cl6 parasites line[28] by double cross-over recombination.

Generation and analysis of Δmsp7 and Δpm4/Δmsp7 parasite lines. The DNA plasmid pRSmsp7-tgdhfr/ts designed to target the *msp7* locus of *P. berghei* ANKA strain contains the following elements (Figure 1A): i) a 5′UTR 485 bp PCR fragments of the *msp7* gene (sense: 5′-CCGGGCCCGCGGGCTAGATTTAATCAGCAATTTGTC; *Apa*I site is underline and antisense: 5′-CCATCGATTTTGTCTAAATATATGTGTGTGTATG; *Cla*I site is underline); ii) a 3′UTR 375 bp PCR fragments (sense: 5′-GGAATTCATTATGTACACAGGAAATACATATAAAAC; *Eco*RI site is underline and antisense: 5′-CGGGATCCCAATGTTACCGAAGAAAAATACAAAC; *BamH*I site is underline); iii) the *Toxoplasma gondii* dihydrofolate reductase/thymidylate synthase (*tgdhfr/ts*) selectable marker cassette. The plasmid was linearised with *Sac*II and used for the generation of mutant lines Δmsp7 cl7, Δmsp7 cl8 and Δmsp7$^+$ as described below[59]. The structure of the *msp7* locus in transformed and wt parasites was analyzed in PCR experiments (Figure 1B) using primer pair 1+2 (n.1: 5′-ATGATGGCATATAAAAAGTTA TGTTTTTTA G; n.2: 5′-TTATTTAAGATCAACTGTAGCTAAGG) under conditions where the *msp7* sequence is readily amplified from pbwt (Figure 1B). The expected integration into the *msp7* locus was verified by successfully amplifying the predicted 5′ and 3′ boundary sequences using primer pairs 3+4 (n.3: 5′-ACTGGAGCAACATGCGGAC; n.4: 5′- CAAACATACAAAAATAAACACC) and 5+6 (n.5: 5′- TATATAATTTGTGAGGGATATG; n.6: 5′-GTCGTATTCCCAATATTTACTAC) as shown in Figure 1B. For RT-PCR total RNA from mixed blood-stage parasites was extracted using TRIzol reagent (Invitrogen) and treated with TURBO DNase (Ambion). cDNA synthesis was performed using the Super script III Platinum two-step qRT-PCR kit (Invitrogen). The amplification of *msp7* gene was performed with primer pair 1+2 (see Figure 1A) and as a control the tubulin gene was amplified with

the following primers: sense 5′-TGGAGCAGGAAATAACTGGG and antisense 5′-ACCTGACATAGCGGCTGAAA (Figure 1C and S1C). The lack of MSP7 expression was confirmed by immunofluorescence experiments using anti-PbMSP7 antibody raised in a mouse immunized with the recombinant protein. For protein expression a region of the *msp7* coding sequence was amplified with the following primers: sense 5′-CACCATGATGGCATATAAAAAGTTATGTTTTTTAG and antisense 5′-TTATTTAAGATCAACTGTAGCTAAGG and cloned into pEXP1-DEST Gateway® Invitrogen vector. Cell lines BL21 Star® pLysS (Invitrogen) were transformed and the recombinant protein purified by Ni-NTA Spin Kit (Qiagen) after IPTG (1mM) induction. Female BALB/c mice were immunized four times with 50 μg of purified protein. The sera from immunized mice was analyzed by immuno-microarray technology (data not shown) and used in immunofluorescence assay at 1 : 500 dilution. Antibody bound to the blood-stage parasites was visualized following incubation with a secondary antibody goat anti-mouse (FITC conjugated) (Figure 1D). VECTASHIELD Mounting Medium with DAPI (Vector) Labs) was used to stain the nuclei of parasites. The images were captured by Nikon Eclipse TE2000-U microscopy and analyzed with NIS-Elements imaging software. The DNA plasmid pRSpm7-hdhfr (Figure S1A), designed to target the *msp7* locus in the Δpm4 cl6 background parasites (that already contain the *tgdhfr/ts* selectable marker used for the deletion of *pm4* gene), was obtained from plasmid pRSpm7-tgdhfr/ts by the exchange of *tgdhfr/ts* selectable marker cassette with the human dihydrofolate reductase (*hdhfr*) selectable marker cassette. The *hdhfr* cassette was obtained from plasmid pL0008 (MR4) by *Pst*I and *Eco*RI digestion and cloned into the plasmid pRSpm7-tgdhfr/ts. The plasmid was linearized with *Sac*II and used for the generation of mutant lines Δpm4/Δmsp7 cl4 and Δpm4/Δmsp7 cl12. The disruption of the *msp7* locus by plasmid pRSpm7-hdhfr in these parasites line was analyzed by PCR reaction using primer pair 1+2 as describe above (Figure 1SB). Integration specific PCR was performed to confirm plasmid insertion in the *msp7* locus using primers pair: 3+7 (n. 3 as above; n.7: 5′-AGCACAATATCTAGGATACTAC) to analyze the 5′UTR integration site and primer pair 8+6 (n. 6 as above; n. 8: 5′-ATGGTTGGTTCGCT-AAACTGCATCG) to investigate the 3′UTR integration site (Figure S1B). For the generation of all mutant lines blood-stages parasites were transfected with 5–10 μg of gel-purified DNA linear fragments and mutant parasites were obtained by the standard method of drug selection by pyrimethamine or WR92210 (kindly provided by Jacobus Pharmaceutical Company) in mice [59]. We enriched the recombinant genotype in the parental transfected parasites population after at least four repeated drug selection treatments until no wild-type genotype was detectable by genomic PCR. Resistant parasites were subsequently cloned by limiting dilution as previously described[59].

Monitoring of parasite infection. The course of infection in BALB/c mice, which are not susceptible to ECM, was analyzed after either intraperitoneal (i.p) or intravenously (i.v) inoculations of 10^7 or 50 infected red blood cells (iRBCs) respectively. The parasitemia (=% of infected erythrocytes) was determined by counting daily Giemsa stained slides of tail blood. Challenge experiments were carried out by i.v. injection of pbwt or *P. yoelii* 17X iRBCs.

Assessment of ECM. The development of cerebral complications was analyzed in C57BL/6 and CD1 mice that are susceptible to ECM. This condition in *P. berghei* is well characterized and defined as the development of cerebral complications (drop in body temperature <34°C, ataxia, paralysis, convulsions, coma) at day 6–9 after infection of mice with 10^4 to 10^6 parasites[2,37]. In this study mice were injected i.p. with 10^5 iRBCs (Δmsp7 and Δpm4/Δmsp7 infected mice were also infected with higher dose (10^6 to 10^7) because of the low growth rate of parasites). The onset of cerebral complications was determined by observing several clinical signs such as ruffled fur, hunching, limb paralysis, coma and by measuring the drop in body temperature at day 5–8 after infection. The body temperature was measured using a 2 Channel Thermometer TK 98802 (2 Biological Instruments) with a rectal probe for mice. A drop in temperature below 34°C is indicative of cerebral complications[36].

For the analysis of blood-brain-barrier (BBB) damage and vascular permeability C57BL/6 mice 7 days post infection had been injected i.v. with 2% Evans Blue[60]. Two hours after dye injection the mice were perfused with heparinized PBS. The brain were dissected, weighted, digital image collected, frozen in LN_2, and stored at −80°C. Brain samples were homogenized in 1 mL of 50% trichloroacetic acid and stored overnight at 4°C. The supernatant was obtained by centrifugation at 21.000 *g* for 30 minutes. The amount of Evans Blue dye was measured by a microplate reader (excitation 600 nm, emission 650 nm) and quantified according to a standard curve. Results are expressed as ng of Evans Blue per mg of brain tissue. Bioluminescence analysis and signal quantification from brain of C57BL/6 mice with asynchronous infection at day 7 post injection was performed after extensive intracardiac perfusion of the animals with heparinized PBS by *in vivo* Imaging System (IVIS 200, Xenogen) as described[28]. Imaging data were analyzed using the programs LIVING IMAGE (Xenogen) and IGOR PRO (WaveMetrics).

Analysis of parasite distribution in live animals and isolated organs. Sequestration of schizonts in whole bodies of live CD1 mice and isolated organs was visualized through imaging of luciferase-expressing, transgenic parasites with an intensified-charge-coupled device (I-CCD) photon counting video camera of the *in vivo* Imaging System (IVIS200 Xenogen) as described[38,39]. Sequestration patterns were monitored in mice with synchronized infections of schizonts. Infections (1–3% parasitemia) were established by injection of cultured, purified schizonts. Imaging was performed between 17h and 23h after injection of schizonts. Imaging of individual organs, obtained by dissection from animals at 21h, was done as described previously[38]. Imaging data were analyzed by using the programs LIVING IMAGE (Xenogen) and IGOR PRO (WaveMetrics).

Statistical analyses. Differences in survival of different groups were analysed using the Kaplan-Meier log-rank test. Differences in the parasitemia and bioluminescence were performed using the Mann-Whitney nonparametric test. For all statistical test, $p<0.05$ was considered significant. In all figures, *, **, *** denote p value of $p<0.05$, $p<0.01$ e $p<0.001$ respectively.

1. Grau, G. E., Piguet, P. F., Vassalli, P. & Lambert, P. H. Tumor-necrosis factor and other cytokines in cerebral malaria: experimental and clinical data. *Immunol Rev.* **112**, 49–70 (1989).
2. Engwerda, C., Belnoue, E., Gruner, A. C. & Renia, L. Experimental models of cerebral malaria. *Curr Top Microbiol Immunol.* **297**, 103–43 (2005).
3. van der Heyde, H. C., Nolan, J., Combes, V., Gramaglia, I. & Grau, G. E. A unified hypothesis for the genesis of cerebral malaria: sequestration, inflammation and hemostasis leading to microcirculatory dysfunction. *Trends Parasitol.* **22**, 503–8 (2006).
4. Sein, K. K., Maeno, Y., Thuc, H. V., Anh, T. K. & Aikawa, M. Differential sequestration of parasitized erythrocytes in the cerebrum and cerebellum in human cerebral malaria. *Am J Trop Med Hyg.* **48**, 504–11 (1993).
5. Brabin, B. J. *et al.* The sick placenta-the role of malaria. *Placenta.* **25**, 359–78 (2004).
6. Schofield, L. Intravascular infiltrates and organ-specific inflammation in malaria pathogenesis. *Immunol Cell Biol.* **85**, 130–7 (2007).
7. Rogerson, S. J., Hviid, L., Duffy, P. E., Leke, R. F. & Taylor, D. W. Malaria in pregnancy: pathogenesis and immunity. *Lancet Infect Dis* **7**, 105–17 (2007).
8. Nunes, M. C. & Scherf, A. *Plasmodium falciparum* during pregnancy: a puzzling parasite tissue adhesion tropism. *Parasitology.* **134**, 1863–9 (2007).
9. Newbold, C. I. *et al.* PfEMP1, polymorphism and pathogenesis. *Ann Trop Med Parasitol.* **91**, 551–7 (1997).
10. Kraemer, S. M. & Smith, J. D. A family affair: var genes, PfEMP1 binding, and malaria disease. *Curr Opin Microbiol.* **9**, 374–80 (2006).
11. Fairhurst, R. M. & Wellems, T. E. Modulation of malaria virulence by determinants of *Plasmodium falciparum* erythrocyte membrane protein-1 display. *Curr Opin Hematol* **13**, 124–30 (2006).
12. Gardiner, D. L., Skinner-Adams, T. S., Spielmann, T. & Trenholme, K. R. Malaria transfection and transfection vectors. *Trends Parasitol.* **19**, 381–3 (2003).
13. Balu, B. & Adams, J. H. Functional genomics of *Plasmodium falciparum* through transposon-mediated mutagenesis. *Cell Microbiol* **8**, 1529–36 (2006).
14. Balu, B. & Adams, J. H. Advancements in transfection technologies for *Plasmodium*. *Int J Parasitol* **37**, 1–10 (2007).
15. Garcia, C. R. *et al. Plasmodium* in the postgenomic era: new insights into the molecular cell biology of malaria parasites. *Int Rev Cell Mol Biol.* **266**, 85–156 (2008).
16. Baldi, D. L. *et al.* RAP1 controls rhoptry targeting of RAP2 in the malaria parasite *Plasmodium falciparum*. *Embo J* **19**, 2435–43 (2000).
17. Triglia, T. *et al.* Apical membrane antigen 1 plays a central role in erythrocyte invasion by *Plasmodium* species. *Mol Microbiol* **38**, 706–18 (2000).
18. Baldi, D. L., Good, R., Duraisingh, M. T., Crabb, B. S. & Cowman, A. F. Identification and disruption of the gene encoding the third member of the low-molecular-mass rhoptry complex in *Plasmodium falciparum*. *Infect Immun* **70**, 5236–45 (2002).
19. Miller, S. K. *et al.* A subset of *Plasmodium falciparum* SERA genes are expressed and appear to play an important role in the erythrocytic cycle. *J Biol Chem* **277**, 47524–32 (2002).
20. Klemba, M., Gluzman, I. & Goldberg, D. E. A *Plasmodium falciparum* dipeptidyl aminopeptidase I participates in vacuolar hemoglobin degradation. *J Biol Chem* **279**, 43000–7 (2004).
21. Black, C. G., Wu, T., Wang, L., Topolska, A. E. & Coppel, R. L. MSP8 is a non-essential merozoite surface protein in *Plasmodium falciparum*. *Mol Biochem Parasitol* **144**, 27–35 (2005).
22. Janse, C. J. *et al.* Malaria parasites lacking *eef1*a have a normal S/M phase yet grow more slowly due to a longer G1 phase. *Mol Microbiol.* **50**, 1539–51 (2003).
23. Tewari, R., Ogun, S. A., Gunaratne, R. S., Crisanti, A. & Holder, A. A. Disruption of *Plasmodium berghei* merozoite surface protein 7 gene modulates parasite growth *in vivo*. *Blood.* **105**, 394–6 (2005).
24. Thompson, J. *et al. Plasmodium* cysteine repeat modular proteins 1–4: complex proteins with roles throughout the malaria parasite life cycle. *Cell Microbiol.* **9**, 1466–80 (2007).
25. de Koning-Ward, T. F., Drew, D. R., Chesson, J. M., Beeson, J. G. & Crabb, B. S. Truncation of *Plasmodium berghei* merozoite surface protein 8 does not affect *in vivo* blood-stage development. *Mol Biochem Parasitol* **159**, 69–72 (2008).
26. Bonilla, J. A. *et al.* Effects on growth, hemoglobin metabolism and paralogous gene expression resulting from disruption of genes encoding the digestive vacuole plasmepsins of *Plasmodium falciparum*. *Int J Parasitol.* **37**, 317–27 (2007).
27. Kadekoppala, M., O'Donnell, R. A., Grainger, M., Crabb, B. S. & Holder, A. A. Deletion of the *Plasmodium falciparum* merozoite surface protein 7 gene impairs parasite invasion of erythrocytes. *Eukaryot Cell.* **7**, 2123–32 (2008).

28. Spaccapelo, R. *et al.* Plasmepsin 4-deficient *Plasmodium berghei* are virulence attenuated and induce protective immunity against experimental malaria. *Am J Pathol* **176**, 205–17 (2010).
29. Mello, K. *et al.* A multigene family that interacts with the amino terminus of *Plasmodium* MSP-1 identified using the yeast two-hybrid system. *Eukaryot Cell.* **1**, 915–25 (2002).
30. Kadekoppala, M., Ogun, S. A., Howell, S., Gunaratne, R. S. & Holder, A. A. Systematic genetic analysis of the *Plasmodium falciparum* MSP7-like family reveals differences in protein expression, location, and importance in asexual growth of the blood-stage parasite. *Eukaryot Cell* **9**, 1064–74 (2010).
31. Franke-Fayard, B. *et al.* Murine malaria parasite sequestration: CD36 is the major receptor, but cerebral pathology is unlinked to sequestration. *Proc Natl Acad Sci U S A.* **102**, 11468–73 (2005).
32. Stevenson, M. M. & Riley, E. M. Innate immunity to malaria. *Nat Rev Immunol.* **4**, 169–80 (2004).
33. Urban, B. C., Ing, R. & Stevenson, M. M. Early interactions between blood-stage *plasmodium* parasites and the immune system. *Curr Top Microbiol Immunol.* **297**, 25–70 (2005).
34. Langhorne, J., Ndungu, F. M., Sponaas, A. M. & Marsh, K. Immunity to malaria: more questions than answers. *Nat Immunol.* **9**, 725–32 (2008).
35. Stephens, R. & Langhorne, J. Priming of CD4+ T cells and development of CD4+ T cell memory; lessons for malaria. *Parasite Immunol.* **28**, 25–30 (2006).
36. Curfs, J. H., van der Meide, P. H., Billiau, A., Meuwissen, J. H. & Eling, W. M. *Plasmodium berghei*: recombinant interferon-gamma and the development of parasitemia and cerebral lesions in malaria-infected mice. *Exp Parasitol.* **77**, 212–23 (1993).
37. Hunt, N. H. & Grau, G. E. Cytokines: accelerators and brakes in the pathogenesis of cerebral malaria. *Trends Immunol.* **24**, 491–9 (2003).
38. Franke-Fayard, B., Waters, A. P. & Janse, C. J. Real-time *in vivo* imaging of transgenic bioluminescent blood stages of rodent malaria parasites in mice. *Nat Protoc.* **1**, 476–85 (2006).
39. Pamplona, A. *et al.* Heme oxygenase-1 and carbon monoxide suppress the pathogenesis of experimental cerebral malaria. *Nat Med.* **13**, 703–10 (2007).
40. Ting, L. M., Gissot, M., Coppi, A., Sinnis, P. & Kim, K. Attenuated *Plasmodium yoelii* lacking purine nucleoside phosphorylase confer protective immunity. *Nat Med.* **14**, 954–8 (2008).
41. Aly, A. S., Downie, M. J., Mamoun, C. B. & Kappe, S. H. Subpatent infection with nucleoside transporter 1-deficient *Plasmodium* blood stage parasites confers sterile protection against lethal malaria in mice. *Cell* **12**, 930–8 (2010).
42. Legorreta-Herrera, M., Ventura-Ayala, M. L., Licona-Chavez, R. N., Soto-Cruz, I. & Hernandez-Clemente, F. F. Early treatment during a primary malaria infection modifies the development of cross immunity. *Parasite Immunol.* **26**, 7–17 (2004).
43. Elliott, S. R., Kuns, R. D. & Good, M. F. Heterologous immunity in the absence of variant-specific antibodies after exposure to subpatent infection with blood-stage malaria. *Infect Immun.* **73**, 2478–85 (2005).
44. Belnoue, E. *et al.* Vaccination with live *Plasmodium yoelii* blood stage parasites under chloroquine cover induces cross-stage immunity against malaria liver stage. *J Immunol.* **181**, 8552–8 (2008).
45. Pombo, D. J. *et al.* Immunity to malaria after administration of ultra-low doses of red cells infected with *Plasmodium falciparum*. *Lancet.* **360**, 610–7 (2002).
46. Roestenberg, M. *et al.* Protection against a malaria challenge by sporozoite inoculation. *N Engl J Med.* **361**, 468–77 (2009).
47. Amante, F. H. *et al.* A role for natural regulatory T cells in the pathogenesis of experimental cerebral malaria. *Am J Pathol.* **171**, 548–59 (2007).
48. Nie, C. Q. *et al.* IP-10-mediated T cell homing promotes cerebral inflammation over splenic immunity to malaria infection. *PLoS Pathog.* **5**, e1000369 (2009).
49. McCarthy, J. S. & Good, M. F. Whole parasite blood stage malaria vaccines: a convergence of evidence. *Hum* **6**, 114–23 (2010).
50. Luke, T. C. & Hoffman, S. L. Rationale and plans for developing a non-replicating, metabolically active, radiation-attenuated *Plasmodium falciparum* sporozoite vaccine. *J Exp Biol.* **206**, 3803–8 (2003).
51. Matuschewski, K. Vaccine development against malaria. *Curr Opin Immunol.* **18**, 449–57 (2006).
52. Mikolajczak, S. A., Aly, A. S. & Kappe, S. H. Preerythrocytic malaria vaccine development. *Curr Opin Infect Dis.* **20**, 461–6. (2007).
53. Renia, L., Gruner, A. C., Mauduit, M. & Snounou, G. Vaccination against malaria with live parasites. *Expert Rev Vaccines.* **5**, 473–81 (2006).
54. Vaughan, A. M., Wang, R. & Kappe, S. H. Genetically engineered, attenuated whole-cell vaccine approaches for malaria. *Hum* **6**, 107–13 (2010).
55. Purcell, L. A., Yanow, S. K., Lee, M., Spithill, T. W. & Rodriguez, A. Chemical attenuation of *Plasmodium berghei* sporozoites induces sterile immunity in mice. *Infect Immun.* **76**, 1193–9 (2008).
56. Ishino, T., Chinzei, Y. & Yuda, M. Two proteins with 6-cys motifs are required for malarial parasites to commit to infection of the hepatocyte. *Mol Microbiol.* **58**, 1264–75 (2005).
57. van Dijk, M. R. *et al.* Genetically attenuated, P36p-deficient malarial sporozoites induce protective immunity and apoptosis of infected liver cells. *Proc Natl Acad Sci U S A.* **102**, 12194–9 (2005).
58. Labaied, M. *et al. Plasmodium yoelii* sporozoites with simultaneous deletion of P52 and P36 are completely attenuated and confer sterile immunity against infection. *Infect Immun.* **75**, 3758–68 (2007).
59. Janse, C. J., Ramesar, J. & Waters, A. P. High-efficiency transfection and drug selection of genetically transformed blood stages of the rodent malaria parasite *Plasmodium berghei*. *Nat Protoc.* **1**, 346–56 (2006).
60. Benchenane, K. *et al.* Oxygen glucose deprivation switches the transport of tPA across the blood-brain barrier from an LRP-dependent to an increased LRP-independent process. *Stroke.* **36**, 1065–70 (2005).

Acknowledgments

We thank MR4 for providing us with plasmid pL0008 (MRA-797) and *P. yoelii* 17X (MRA-426). We also thank Chris Janse for providing 1037cl1 parasite line. This work was supported by grants of the Italian Ministry of Research FIRB (Basic Research Investments Programme). The funders had no role in study design, data collection and analysis, decision to publish, or preparation on the manuscript.

Author contributions

RS, designed and performed research, analyzed data, wrote the paper; EA, SC, PA, BC, performed research, analyzed data; MR, FB, intellectually contributed to the work; MDC, TD, analyzed data; AC, designed research, analyzed data and wrote the paper.

Additional information

Supplementary Information accompanies this paper at http://www.nature.com/scientificreports

Competing financial interests: The authors declare no competing financial interests.

License: This work is licensed under a Creative Commons Attribution-NonCommercial-NoDerivative Works 3.0 Unported License. To view a copy of this license, visit http://creativecommons.org/licenses/by-nc-nd/3.0/

How to cite this article: Spaccapelo, R. *et al.* Disruption of plasmepsin-4 and merozoites surface protein-7 genes in *Plasmodium berghei* induces combined virulence-attenuated phenotype. *Sci. Rep.* **1**, 39; DOI:10.1038/srep00039 (2011).